УДК 551.465

© *Н. П. Кузьмина**, *Н. В. Журбас*, 2021
Институт океанологии им. П.П. Ширшова РАН, 117997, Нахимовский пр., д. 36, г. Москва, Россия
*E-mail: kuzmina@ocean.ru

СИММЕТРИЧНАЯ НЕУСТОЙЧИВОСТЬ ГЕОСТРОФИЧЕСКИХ ТЕЧЕНИЙ С КОНЕЧНЫМ ПОПЕРЕЧНЫМ МАСШТАБОМ

Статья поступила в редакцию 30.04.2021, после доработки 23.09.2021

Проведен сравнительный анализ симметричных неустойчивых возмущений геострофического течения с постоянным вертикальным и горизонтальным сдвигом скорости в безграничной области и области с боковыми границами. Представлены расчеты скорости роста неустойчивых возмущений в зависимости от вертикального волнового числа для различных безразмерных параметров задачи. Отмечается, что в случае симметричной неустойчивости течения с конечным поперечным масштабом с учетом диффузии массы и импульса, которая возникает при условии $\mathrm{Ri} \cdot (1 + \mathrm{Ro}) < 1$ (Ri — геострофическое число Ричардсона, Ro — число Россби), существует конечный вертикальный масштаб максимально растущего возмущения в отличие от случая симметричной неустойчивости в безграничной области, когда максимально растущее возмущение с учетом диффузии массы и импульса реализуются при $m \to 0$ (m — вертикальное волновое число). Показано, что совместный эффект боковых границ и диффузии импульса и массы при $\mathrm{Pr} \geq 1$ (Pr — число Прандтля) в зависимости от значений безразмерных параметров задачи может существенно влиять на динамику симметричных возмущений, а именно: приводить к сужению спектра неустойчивых возмущений и уменьшению их скорости роста, и даже препятствовать развитию неустойчивости.

Ключевые слова: симметричная неустойчивость, метод малых возмущений, задача на собственные значения, диффузия массы и импульса, условия неустойчивости геострофического течения.

© *N. P. Kuzmina**, *N. V. Zhurbas*, 2021
Shirshov Institute of Oceanology, Russian Academy of Sciences, 117997, Nahimovskiy prospekt, 36, Moscow, Russia
*E-mail: kuzmina@ocean.ru

SYMMETRIC INSTABILITY OF GEOSTROPHIC CURRENTS WITH A FINITE TRANSVERSE LENGTHSCALE

Received 30.04.2021, in final form 23.09.2021

A comparative analysis of unstable symmetric perturbations of the geostrophic current with a constant vertical and horizontal velocity shear in an unbounded region and a region with lateral boundaries is performed accounting for vertical diffusion of buoyancy and momentum. Calculations of the growth rate of unstable perturbations are presented as a function of the vertical wavenumber for various dimensionless parameters of the problem. It is found that in the case of the geostrophic current with lateral boundaries, the maximum-growing mode of symmetric instability arising when condition $\mathrm{Ri} \cdot (1 + \mathrm{Ro}) < 1$ (Ri is the geostrophic Richardson number, Ro is the Rossby number) is satisfied has a finite vertical length scale, while in the case of the unbounded region, the vertical wavenumber of the maximum-growing mode is asymptotically vanishing. A combined effect of lateral boundaries and diffusion of buoyancy and momentum at $\mathrm{Pr} \geq 1$ (Pr is the Prandtl number), depending on the values of the dimensionless parameters of the problem, can significantly affect the dynamics of symmetric perturbations, namely, lead to a narrowing of the spectrum of unstable perturbations and a decrease in their growth rates, and even prevent the development of instability.

Key words: symmetric instability, small perturbation method, eigenvalue problem, diffusion of mass and momentum, conditions for instability of geostrophic current.

1. Introduction

The study of the instability of geostrophic currents is important for describing the formation of intrusive layering [1–7], generation of eddies [8, 9], exchange, mixing, and transformation of waters in the ocean [10–14]. The study of symmetric instability of baroclinic currents in the upper layer of the ocean [15–18], which can significantly

Ссылка для цитирования: *Кузьмина Н.П.*, *Журбас Н.В.* Симметричная неустойчивость геострофических течений с конечным поперечным масштабом // Фундаментальная и прикладная гидрофизика. 2021. Т. 14, № 4. С. 3–13. doi: 10.7868/S2073667321040018

For citation: *Kuzmina N.P.*, *Zhurbas N.V.* Symmetric Instability of Geostrophic Currents with a Finite Transverse Lengthscale. *Fundamentalnaya i Prikladnaya Gidrofizika*. 2021, 14, 4, 3–13. doi: 10.7868/S2073667321040018

contribute to re-stratification and mixing, has been of particular interest recently. The description of such instability is carried out, as a rule, in the approximation of an ideal fluid. However, in the general case, the term "symmetric instability" is understood as two-dimensional instability (2D instability) of a geostrophic current or front, that is, perturbations are considered that do not depend on the coordinate directed along the flow. Therefore, the McIntyre instability arising due to the difference between buoyancy and momentum diffusivities [19], as well as the instability of baroclinic fronts caused by double diffusion [1–3], should also be attributed to symmetric instability. For convenience, we will refer the 2D instability of the geostrophic flow of an ideal fluid as "classical symmetric instability".

For the first time, probably, the description of the classical symmetric instability for a geostrophic current with a linear vertical profile was performed by Stone [20]. In this work, a criterion for the instability is given $\frac{N^2}{\left(\frac{dU}{dz}\right)^2} = \frac{f^2}{(\alpha N)^2} = \mathrm{Ri} < 1$, where N is the buoyancy frequency, f is the Coriolis parameter, $U(z)$ is the geostrophic current velocity, $\frac{dU}{dz}$ is the constant vertical shear of geostrophic velocity, α is the slope of isopycnal surfaces, Ri is the geostrophic Richardson number. If the constant horizontal gradient of geostrophic velocity $\frac{dU}{dy}$ is taken into account (where y is the transverse coordinate relative to the current), the classical symmetric instability criterion $\mathrm{Ri} < 1$ can be re-written as $\mathrm{Ri} \cdot (1 + \mathrm{Ro}) < 1$, where $\mathrm{Ro} = \left(-\frac{dU}{dy}\right) / f$ is the gradient Rossby number [21].

The analytical description of the classical symmetric instability is limited to considering either an infinite region vertically and horizontally, or a vertically finite and horizontally infinite region (see, for example, [15, 22]). However, ocean fronts or currents have a finite transverse scale. In this regard, it is important to evaluate the possibility of the appearance of symmetric instabilities of various types in the region with lateral boundaries, taking into account vertical diffusion of buoyancy and momentum which is the objective of this study.

2. Description of the problem

The analysis of symmetric instability is carried out for a zonal geostrophic current with a linear vertical velocity profile based on the method of small perturbations. The equations for the mean state are:

$$fU = -\frac{\partial \overline{P}}{\partial y},\ V = 0,\ W = 0,\ \frac{\partial \overline{P}}{\partial z} = -\mathrm{g}\overline{\rho},$$

where U, V, W are the zonal, meridional and vertical velocities of the mean state current; $\overline{P}$, $\overline{\rho}$ are the mean state pressure and density, normalized to the reference density, the x, y and z axes are directed along the current, across the current and upward, respectively. The barotropic shear of the basic flow is taken into account: $U = U(y, z)$, $\partial U/\partial y = \mathrm{const}$.

The equations for small perturbations independent of the x — coordinate (symmetric perturbations), taking into account the vertical diffusion of mass and momentum, will have the following form:

$$\frac{\partial u}{\partial t} - fv + v\frac{\partial U}{\partial y} + w\frac{\partial U}{\partial z} = \mathrm{Pr} \cdot K\frac{\partial^2 u}{\partial z^2}, \tag{1}$$

$$\frac{\partial v}{\partial t} + fu = -\frac{\partial p}{\partial y} + \mathrm{Pr} \cdot K\frac{\partial^2 v}{\partial z^2}, \tag{2}$$

$$\mathrm{g}\rho = -\frac{\partial p}{\partial z}, \tag{3}$$

$$\frac{\partial v}{\partial y} + \frac{\partial w}{\partial z} = 0, \tag{4}$$

$$\frac{\partial \rho}{\partial t} + v\frac{\partial \overline{\rho}}{\partial y} + w\frac{\partial \overline{\rho}}{\partial z} = K\frac{\partial^2 \rho}{\partial z^2}, \tag{5}$$

where u, v, w are the zonal, meridional and vertical components of velocity perturbations, p, ρ are the pressure and density perturbations normalized by the reference density, g is the acceleration of gravity, $K = \mathrm{const}$ is the vertical diffusivity of buoyancy, Pr is the Prandtl number. Here we use the simplest parametrization of the mixing coefficients typical for the analytical analysis of instability (see, for example, [19]).

In the case of a geostrophic current with a finite transverse length scale, the solution for any variables of the system (1)—(5) is sought in the form (see, for example, [23]).

$$\psi = \tilde{\psi}(y)e^{\omega t+imz}, \tag{6}$$

where ω is either the decrement coefficient (if $\omega < 0$) or the growth rate (if $\omega > 0$) of the unstable perturbations, and m is the vertical wavenumber; $\omega = 0$ corresponds to the neutral perturbations.

Substituting (6) into the system (1)–(5), we obtain the equation for the meridional velocity component $\tilde{v}(y)$:

$$\frac{d^2\tilde{v}}{dy^2}+i\frac{d\tilde{v}}{dy}\cdot\left(\alpha m+\frac{\alpha\tilde{\omega}}{\omega_{\mathrm{Pr}}}\right)-\tilde{v}\cdot\left(\frac{\omega_{\mathrm{Pr}}\tilde{\omega}}{N^2}m^2+\frac{ff^*}{N^2}\frac{\tilde{\omega}}{\omega_{\mathrm{Pr}}}m^2\right)=0, \tag{7}$$

where $\alpha \approx tg\alpha = g\overline{\rho}_y / N^2$ is the isopycnal slope $(\alpha \ll 1)$, $\omega_{\mathrm{Pr}} = \omega + \mathrm{Pr}Km^2$, $\tilde{\omega} = \omega + Km^2$, $\overline{\rho}_y$ is the mean state horizontal density gradient, normalized by the reference density, $f^* = f - \frac{\partial U}{\partial y}$.

For a flow with a finite transverse lengthscale L, equation (7) is solved under the following boundary conditions:

$$\tilde{v}(y) = 0 \text{ at } y = 0, L. \tag{8}$$

The eigenvalue problem (7), (8) is reduced to finding the roots (that is, the values of ω depending on the wavenumber m) of the following equation:

$$\frac{1}{4}\left(\alpha m+\alpha\frac{m\tilde{\omega}}{\omega_{\mathrm{Pr}}}\right)^2=\frac{\omega_{\mathrm{Pr}}\tilde{\omega}m^2}{N^2}+\frac{ff^*\tilde{\omega}m^2}{\omega_{\mathrm{Pr}}N^2}+\frac{\pi^2n^2}{L^2},\ (n = 1, 2, 3...). \tag{9}$$

A detailed description of the solution to the eigenvalue problem for a second-order equation (7) with constant coefficients can be found, for example, in [23]. The maximum-growing mode is realized at $n = 1$.

In the case of an ideal fluid, equation (9) is reduced to a quadratic equation

$$\omega^2 + ff^* - \alpha^2N^2 + \frac{\pi^2N^2}{L^2m^2} = 0. \tag{10}$$

The instability condition according to equation (10) is determined by the inequality

$$\alpha^2 - \frac{ff^*}{N^2} > 0 \text{ or } \mathrm{Ri}\cdot(1 + \mathrm{Ro}) < 1, \tag{11}$$

which is the same as in the case of laterally unbounded current (see, e.g. [21] and the Appendix, Section "Ideal fluid"). However, it follows from Eq. (10) that when the condition (11) is satisfied, the perturbations at small wavenumbers can be stable, in contrast to the case of unbounded flow. Thus, the lateral boundaries make the range of unstable wavenumbers narrower, preventing the instability of perturbations with a large vertical scale (or small wavenumber m). It also follows from (10) that the growth rate increases with increasing wavenumber and tends to a maximum value when $m \to \infty$. Here one can see an analogy with the classical symmetric instability for the current without lateral boundaries, but in a layer of finite depth (see e.g. [20]), when the growth rate increases with the growth of the horizontal transverse wavenumber.

For a dissipative fluid at $\mathrm{Pr} = 1$, Eq. (9) has the form

$$\left(\omega + Km^2\right)^2 + ff^* - \alpha^2N^2 + \frac{\pi^2N^2}{L^2m^2} = 0. \tag{12}$$

In this case, the instability condition is also reduced to (11). However, according to (12), perturbations with small and large wave numbers m can be stable. Therefore, due to the presence of lateral boundaries of the flow, as well as due to diffusion of buoyancy and momentum, in this case there is a finite vertical scale of the maximum-growing perturbation (cf. Section "Dissipative fluid" of the Appendix).

For the convenience of calculating Eq. (9) for various values of Pr, we introduce dimensionless variables as follows

$$\omega^* = \frac{\omega}{f},\ m^* = m\left(\frac{K}{f}\right)^{1/2}.$$

Let us rewrite (9) in the dimensionless variables, omitting the "asterisks":

$$\frac{1}{4\mathrm{Ri}}\left(1+\frac{\tilde{\omega}}{\omega_{\mathrm{Pr}}}\right)^2=\omega_{\mathrm{Pr}}\tilde{\omega}+\frac{(1+\mathrm{Ro})\tilde{\omega}}{\omega_{\mathrm{Pr}}}+\frac{\pi^2}{m^2}\mathrm{Bu}^*, \tag{13}$$

where $\omega_{\mathrm{Pr}}=\omega+\mathrm{Pr}m^2$, $\tilde{\omega}=\omega+m^2$, and $\mathrm{Bu}^*=\frac{K}{f}\frac{N^2}{f^2L^2}=\frac{h^2}{f^2}\frac{N^2}{L^2}$ is an analogue of the Burger number, $\mathrm{Bu}=\frac{H^2N^2}{f^2L^2}$, which is an important parameter in problems of 3D instability of geostrophic currents with vertical scale, H, and horizontal scale, L (see e.g. [9]); $h=\left(\frac{K}{f}\right)^{1/2}$ is the characteristic vertical scale of the perturbation.

Let us compare the maximum growth rates of unstable perturbations obtained from (13) with those for an unbounded frontal zone (Appendix, Section "Dissipative fluid", Eq. A9).

3. Results of calculations

Unbounded region

In the case of an ideal fluid, the maximum-growing perturbations are parallel to the isopycnic surfaces (see, for example, [15] and Section "Ideal fluid" of the Appendix), and the growth rate does not depend on the wavenumber m (Appendix, formula (A4)). The instability pattern changes if we take into account dissipation (Fig. 1).

In this case, the maximum-growing modes are also parallel to the isopycnals, but, according to calculations for the selected values of the problem parameters, perturbations are stable at $m > 1.2$. The maximum growth rate at these values of the parameters is close to unity, that is, the characteristic time of the formation of perturbations (the increase in the amplitude by a factor of e) at $f = 10^{-4}$ s^{-1} is approximately 3 hours. The instability at Pr = 1 should be distinguished from the classical symmetric instability, despite a similar instability criterion (see Appendix, Section "Dissipative fluid").

Figure 2, *a* shows the ω as a function of vertical wavenumber m at Pr = 10 and different values of Ri and Ro. With the increase of Pr, the region of unstable perturbations becomes much narrower. The growth rate of the maximum-growing perturbations due to the McIntyre instability (Section "Dissipative fluid" of the Appendix) is significantly lower than that for the symmetric instability (curve 3 in Fig. 2, *a*).

An important feature of the McIntyre instability, as well as the instability of the baroclinic front due to double diffusion (see, for example, [3]), is that there is a finite vertical scale (or finite wavenumber) of the maximum-grow-

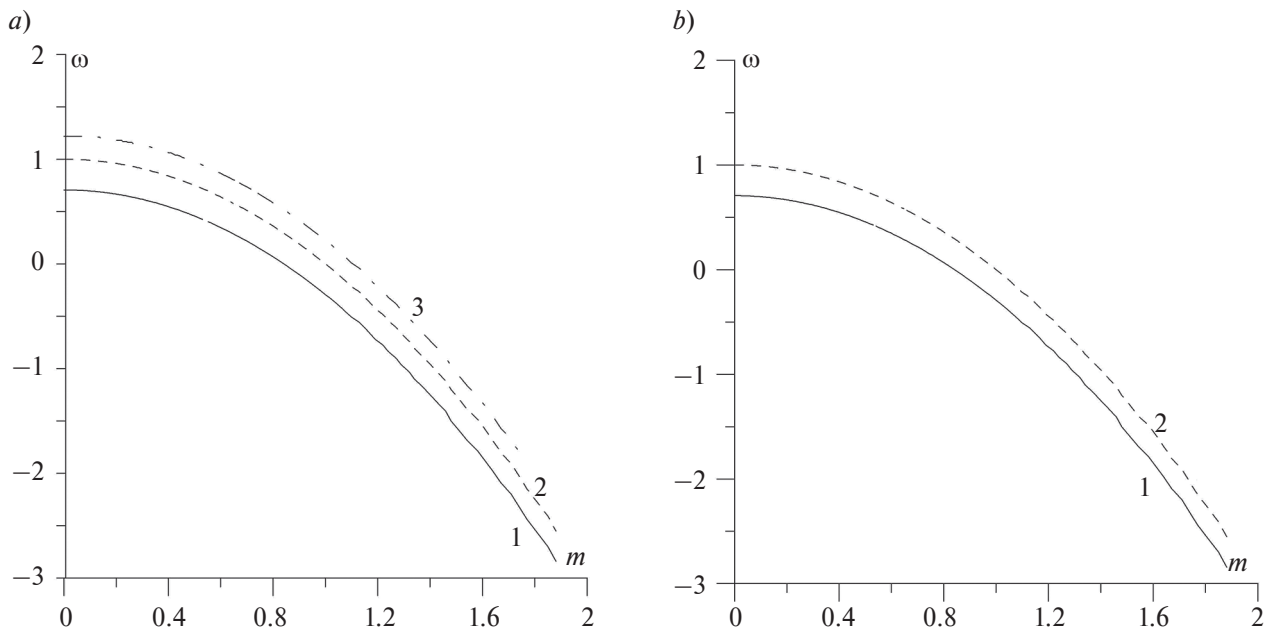

Fig. 1. The ω vs m calculated on the basis of equation (A9) for Pr = 1, and for various values of the problem parameters: *a* — curve 1: Ri = 0.5, Ro = 0.5; curve 2: Ri = 0.5, Ro = 0; curve 3: Ri = 0.5, Ro = –0.5; *b* — curve 1: Ri = 1, Ro = –0.5; curve 2: Ri = 1, Ro = –1.

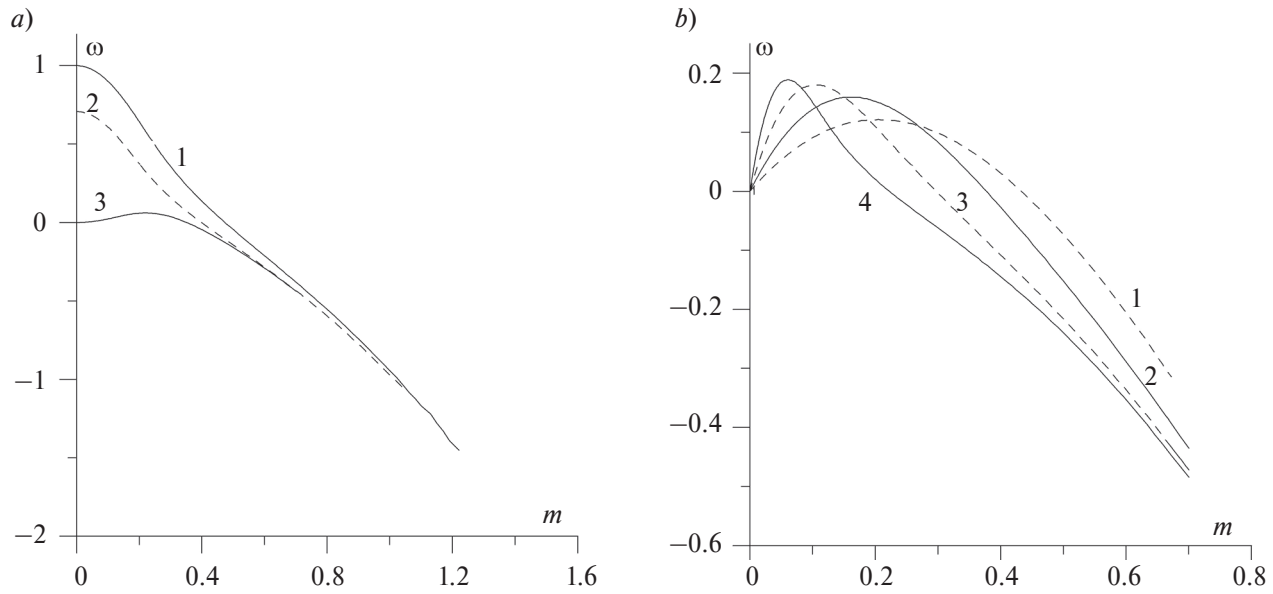

Fig. 2. The ω vs *m* calculated on the basis of equation (A9) for various values of the problem parameters: *a* — Pr =10, curve 1: Ri = 0.5, Ro = 0; curve 2: Ri = 1, Ro = –0.5; curve 3: Ri = 1, Ro = 0.5; *b* — Ri = 1, Ro = 0 (McIntyre instability), curve 1: Pr = 4; curve 2: Pr = 10; curve 3: Pr = 30; curve 4: Pr = 100.

ing perturbation in the infinite region. Figure 2, *b* shows the growth rates for the McIntyre instability at Ri = 1, Ro = 0 and different values of the Pr. With the increase of Pr, the wavenumber of the maximum-growing perturbation decreases, and the growth rate ω weakly increases, but even at high Pr it remains limited as $\omega < 0.2$.

Region with lateral boundaries

The lateral boundaries of the flow contribute to the stability of perturbations at low vertical wavenumbers (Fig. 3, *a*). Due to the combined effect of lateral boundaries and dissipation, there is a maximum-growing perturbation at a finite wavenumber *m* for the symmetric instability arising under the condition (11) (compare Figs 1, *a* and 3, *a*).

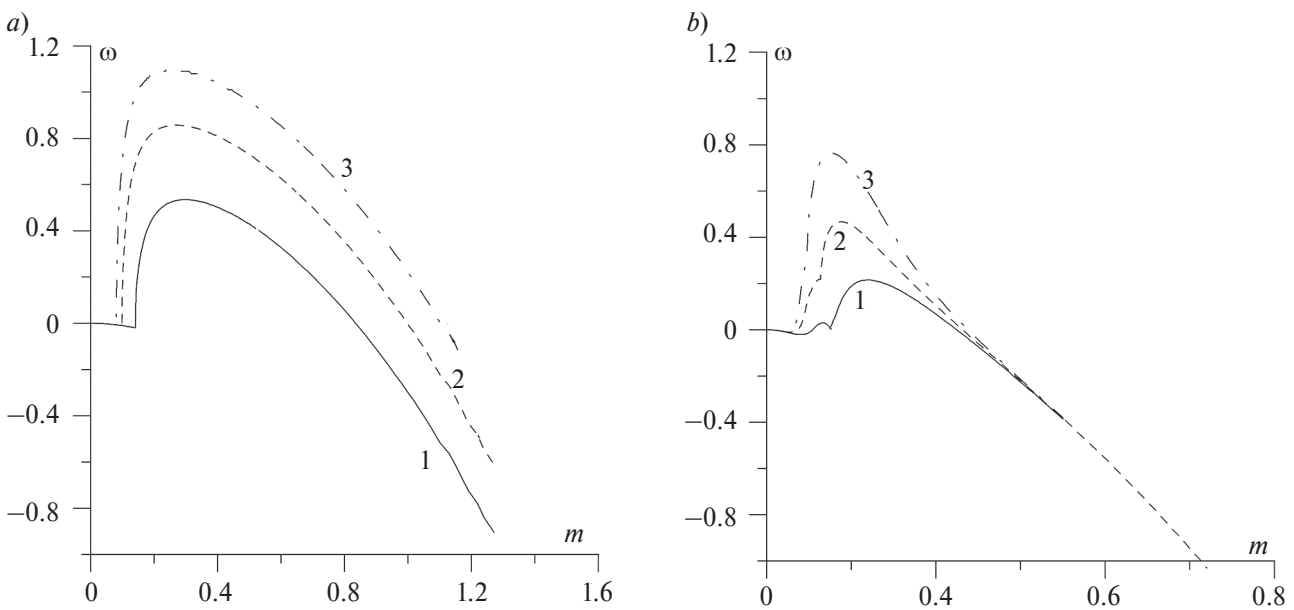

Fig. 3. The ω vs *m* calculated on the basis of equation (13) for various values of the problem parameters at $Bu^* = 0.001$: *a* — Pr = 1; curve 1: Ri = 0.5, Ro = 0.5; curve 2: Ri = 0.5, Ro = 0; curve 3: Ri = 0.5, Ro = — 0.5; *b* — Pr = 10; curve 1: Ri = 0.5, Ro = 0.5; curve 2: Ri = 0.5, Ro = 0; curve 3: Ri = 0.5, Ro = –0.5.

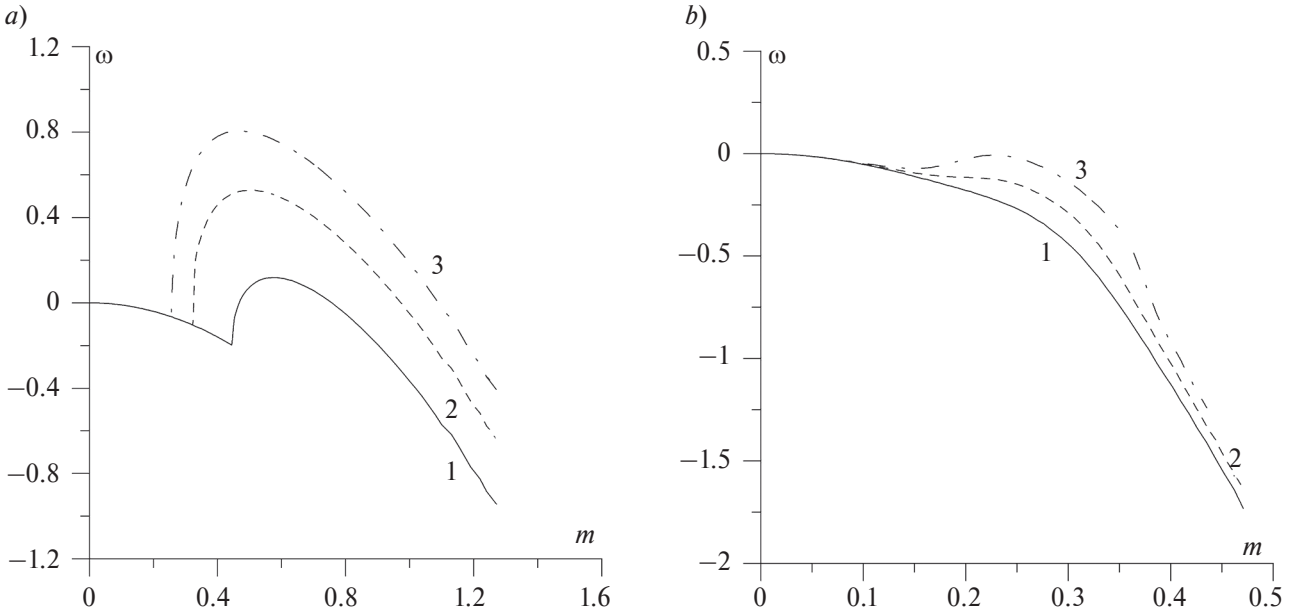

Fig. 4. The same as in Fig. 3, but at Bu* = 0.01.

With the increase of Pr, the growth rate of the symmetric instability arising when condition (11) is satisfied decreases (Fig. 3). Moreover, for certain values of Bu^* and Pr, the symmetric instability does not appear even if condition (11) is satisfied (see Fig. 4, *b*, curves *1* and *2*).

The presence of lateral boundaries of the flow especially sharply affects the McIntyre instability (cf. Figs 2, *b* and 5). With the increase of Pr, the growth rate of the maximum-growing perturbation first increases and then tends to zero (Fig. 5, *a*). For $Bu^* \sim 0.01$, the McIntyre instability does not arise even when Pr = 4 (Fig. 5, *b*). Therefore, the fulfillment of the condition $1 \le Ri < (Pr + 1)^2/4Pr$ does not guarantee the development of McIntyre instability ([19], see also Appendix, Section "Dissipative fluid") in the region with lateral boundaries at some values of Bu^*.

4. Discussion of results and conclusions

First of all, let us briefly discuss the influence of the Prandtl number on the dynamics of perturbations. The geostrophic current or front is stable due to the balance between the velocity field and the density field. This balance can

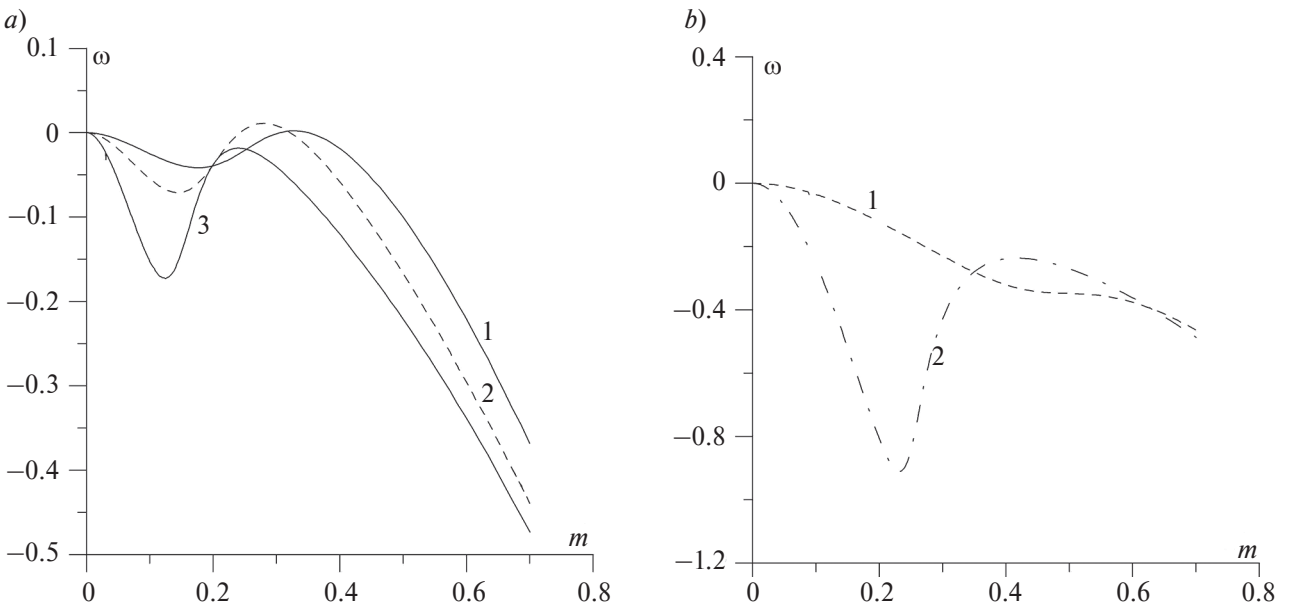

Fig. 5. The ω vs *m* calculated on the basis of equation (13) at Ri = 1, Ro = 0 (McIntyre instability): *a* — $Bu^* = 0.001$; curve 1: Pr = 4; curve 2: Pr = 10; curve 3: Pr = 30; *b* — $Bu^* = 0.01$; curve 1: Pr = 4; curve 2: Pr = 30.

be violated if the momentum diffusion exceeds the mass diffusion (Pr > 1). For this reason, the current or front can come to an unstable state. Obviously, at Pr < 1, an imbalance can also occur between the density field and the velocity field. Therefore, the McIntyre instability is often called viscous-diffusion instability. A detailed explanation of this instability for a geostrophic current without lateral boundaries is given in [24].

Our calculations show that with an increase in the Prandtl number (with increasing friction), the spectrum of short-wave (large m) unstable disturbances narrows. In turn, the lateral boundaries of the front narrow the spectrum of unstable long (small m) perturbations. Thus, the combined effect of friction and lateral boundaries prevents the generation of unstable perturbations on both sides of the spectrum. Therefore, it is physically justified to expect that for some values of the parameters characterizing the mean field, the instability of the geostrophic current with lateral boundaries may not appear taking into account dissipation. An analysis of cases of instability of a front with lateral boundaries at Pr < 1 is beyond the scope of this work. This is primarily due to the fact that the inequality Pr ≥ 1 is typical for the ocean.

According to calculations, the growth rate of unstable perturbations is sensitive to the value of the parameter $\mathrm{Bu}^* = \frac{K}{L^2 f}\frac{N^2}{f^2}$. Therefore, it is important to evaluate the typical values of this parameter in the ocean. The vertical diffusivity K in the ocean lies in a wide range: in the upper quasi-homogeneous layer, K can reach a value comparable to 1 $\mathrm{m^2 s^{-1}}$, while in the pycnocline, where the turbulence has intermittent character, it can be as small as 10^{-6} $\mathrm{m^2 s^{-1}}$ (see, e.g., [4]).

However, we must take into account that the value of K is small at large N. In this regard, there are certain restrictions on the maximum value of the parameter Bu^* even in the cases when currents have a small transverse scale L (about several kilometers). Indeed, setting $\mathrm{Bu}^* = 0.01$, $N = 3 \cdot 10^{-3}$ $\mathrm{s^{-1}}$, $f = 10^{-4}$ $\mathrm{s^{-1}}$, $L = 3 \cdot 10^3$ m we get that the diffusivity should be sufficiently large, $K = 10^{-2}$ $\mathrm{m^2 s^{-1}}$. Thus, it is most likely to suggest that typical values of the Bu^* can rarely exceed 0.01. Nevertheless, even at smaller values of Bu^*, the effect of lateral boundaries and diffusion can significantly reduce the growth rates of symmetric perturbations (see Figs. 3–4) and even totally suppress the instability.

Taking into account that the vertical shear of geostrophic current with a linear vertical profile is expressed as $\frac{dU}{dz} = \frac{N^2 \alpha}{f}$, large values of vertical shear are expected at fronts with high values of the isopycnal slope a and buoyancy frequency N. It is reasonably to estimate α and $\frac{dU}{dz}$ for the selected values of the Richardson number used in our calculations and the following values of the buoyancy frequency and the Coriolis parameter: $N = 3 \cdot 10^{-3}$ $\mathrm{s^{-1}}$, $f = 10^{-4}$ $\mathrm{s^{-1}}$. Taking $\mathrm{Ri} = \frac{f^2}{(N\alpha)^2} = 0.5$, we get $\alpha = 4.7 \cdot 10^{-2}$. Typical mean slopes of isopycnals in the ocean pycnocline, as a rule, are more than an order of magnitude smaller (see, e.g., [11, 23]). However, in the upper quasi-uniform layer, the isopycnal slopes may even exceed the obtained value. Indeed, according to [16], the Ekman transport caused by the wind stress on the ocean surface can significantly increase the isopycnal slopes. Substituting the above values α, N, f into the formula for the vertical shear, we obtain $\frac{dU}{dz} = 4.2 \cdot 10^{-3}$ $\mathrm{s^{-1}}$. If we apply our considerations to a vertical layer of 100 m thick, the maximum current velocity will be equal to 0.42 m $\mathrm{s^{-1}}$, which satisfactorily corresponds to the observed velocities at oceanic fronts.

In conclusion, let us briefly summarize the main results of the study.

A comparative analysis of unstable symmetric perturbation of the geostrophic current with a constant vertical and horizontal velocity shear in an unbounded region and a region with lateral boundaries is performed accounting for vertical diffusion of buoyancy and momentum.

It is found that in the case of the current with lateral boundaries, the maximum-growing mode of symmetric instability arising when condition Ri · (1 + Ro) < 1 is satisfied has a finite vertical length scale, while in the unbounded case, the vertical wavenumber of the maximum-growing mode is asymptotically vanishing.

The combined effect of lateral boundaries and diffusion of buoyancy and momentum at Pr ≥ 1, depending on the values of the dimensionless parameters of the problem, can significantly affect the dynamics of symmetric perturbations, namely, lead to a narrowing of the spectrum of unstable perturbations and a decrease in their growth rates, and even prevent the development of instability.

4. Acknowledgements

The authors are grateful to anonymous reviewers for useful comments.

5. Funding

The work was carried out within the framework of the state assignment of the Shirshov Institute of Oceanology RAS (theme 0128–2021–0001).

Appendix

In the case of infinite area, the solution of system Eq. (1)—(5) is sought in the form

$$\psi = \psi_0 \exp\left(\omega t + imz + ily\right), \tag{A1}$$

where ψ is any disturbed variable from Eq. (1)—(5). Note that with this form of a solution, the tangent of the angle of inclination of the perturbations relative to the horizontal (slope) is $\tan(\gamma) = -\frac{l}{m}$.

Let's consider different cases of the Eq. (1)—(5) for solutions (A1).

Ideal fluid

After removing the last term in the right hand part of Eq. (1), (2), and (5) and substituting Eq. (A1) to Eq. (1)—(5) the following equation for ω is obtained:

$$\omega^2 + ff^* + 2 \cdot \alpha \cdot \mathrm{N}^2 \frac{l}{m} + \mathrm{N}^2 \frac{l^2}{m^2} = 0. \tag{A2}$$

Let's rewrite (A2) as:

$$\omega^2 + ff^* + \mathrm{N}^2 \left(l / \mathrm{m} + \alpha\right)^2 - \alpha^2 N^2 = 0. \tag{A3}$$

It follows from Eq. (A3) that instability (i.e., $\omega > 0$) is possible only when $\alpha^2 - \frac{ff^*}{N^2} > 0$ or $\mathrm{Ri} \cdot (1 + \mathrm{Ro}) < 1$. Thus, we obtain the Hoskins formula [21] (see also Eq. (11)).

According to Eq. (A3), the slope of the maximum growing perturbations, γ_i, is

$$\gamma_i = -\left(\frac{l}{m}\right)_i = \alpha.$$

Thus, perturbations with different wave numbers *m* and *l*, which are parallel to the isopycnic surfaces, have a maximum growth rate (see also [17, 19]).

The growth rate of the maximum growing perturbations, ω_i, is

$$\omega_i = f\left(\frac{1}{\mathrm{Ri}} - \left(1 + \mathrm{Ro}\right)\right)^{1/2}. \tag{A4}$$

Note that Eq. (A4) coincides the well-known formula by Stone [20], provided that Ro = 0. Formula (A4) was also obtained in [15].

Dissipative fluid

In this case the equation for ω at $\alpha \ll 1$ is:

$$\frac{\tilde{\omega}\omega_{\mathrm{Pr}}}{N^2} + \frac{l}{m}\alpha\left(1 + \frac{\tilde{\omega}}{\omega_{\mathrm{Pr}}}\right) + \frac{ff^*}{N^2}\frac{\tilde{\omega}}{\omega_{\mathrm{Pr}}} + \frac{l^2}{m^2} = 0, \tag{A5}$$

where $\omega_{\mathrm{Pr}} = \omega + \mathrm{Pr}Km^2$, $\tilde{\omega} = \omega + Km^2$.

For Pr = 1, Eq. (A5) is reduced to a quadratic equation:

$$\left(\omega + Km^2\right)^2 + ff^* + \mathrm{N}^2\left(\frac{l}{m} + \alpha\right)^2 - \alpha^2 N^2 = 0. \tag{A6}$$

As in the case of the ideal fluid, the instability is possible only if inequality (11) is satisfied. Equation (A6) also implies that the slope of the maximum-growing perturbations is equal to the slope of isopycnic surfaces. However, the maximum-growing perturbation is realized at $m \to 0$ (cf. Eqs. (A3), A(6), and (12)).

For Pr ≠ 1, Eq. (A5) is reduced to a polynomial of the third degree

$$\omega^3 + C_2\omega^2 + C_1\omega + C_0 = 0. \tag{A7}$$

It is easy to show that when the inequality $1 \le \mathrm{Ri}\cdot(1+\mathrm{Ro})$ is satisfied, the coefficients C_2, C_1 are nonnegative. Thus, Eq. (A7) has one and only one positive real root and only if $C_0 < 0$ (see, e.g., [3]).

To analyze the dissipation-related instability, let us consider the free term of Eq. (A7)

$$C_0 = Km^2\mathrm{N}^2\mathrm{Pr}\left(\frac{\mathrm{Pr}Km^4}{N^2}+\frac{ff^*}{\mathrm{Pr}N^2}+\left(\frac{\alpha(\mathrm{Pr}+1)}{2\mathrm{Pr}}+\frac{l}{m}\right)^2-\frac{\alpha^2(\mathrm{Pr}+1)^2}{4\mathrm{Pr}^2}\right). \tag{A8}$$

Coefficient C_0 can be negative only if

$$\frac{ff^*}{\alpha^2N^2} = \mathrm{Ri}(1+\mathrm{Ro}) < \frac{(\mathrm{Pr}+1)^2}{4\mathrm{Pr}}.$$

Conditions $1 \le \mathrm{Ri}(1+\mathrm{Ro}) < \frac{(\mathrm{Pr}+1)^2}{4\mathrm{Pr}}$ and Pr ≠ 1 are the McIntyre instability conditions [19]. The slope of the maximum-growing perturbation according to (A8) is

$$\gamma_i = -\left(\frac{l}{m}\right)_i = \alpha\frac{(\mathrm{Pr}+1)}{2\mathrm{Pr}}.$$

It is easy to show that to calculate the maximum growth rate as a function of the vertical wavenumber m for different values of the parameter Ri, Pr, Ro in the approximation of an infinite frontal zone (unbounded region), one should use equation (13) taking into account the condition $\mathrm{L} \to \infty$

$$\frac{1}{4\mathrm{Ri}}\left(1+\frac{\tilde{\omega}}{\omega_{\mathrm{Pr}}}\right)^2 = \omega_{\mathrm{Pr}}\tilde{\omega}+\frac{(1+\mathrm{Ro})\tilde{\omega}}{\omega_{\mathrm{Pr}}}. \tag{A9}$$

Equation (A9) allows one to find the growth rates of perturbations that have a slope corresponding to the maximum-growing increments. Note that equation (A9) can also be obtained based on equation (A5).

Литература

1. *Кузьмина Н.П.*, *Родионов В.Б.* О влиянии бароклинности на образование термохалинных интрузий в океанских фронтальных зонах // Изв. АН СССР. Физика атмосферы и океана. 1992. Т. 28, № 10–11. С. 1077–1086.
2. *May B.D.*, *Kelley D.E.* Effect of baroclinicity on double-diffusive interleaving // J. Phys. Oceanogr. 2007. V. 27. P. 1997–2008.
3. *Kuzmina N.P.*, *Zhurbas V.M.* Effects of double diffusion and turbulence on interleaving at baroclinic oceanic fronts // J. Phys. Oceanogr. 2000. V. 30. P. 3025–3038.
4. *Кузьмина Н.П.*, *Журбас Н.В.*, *Емельянов М.В.*, *Пыжевич М.Л.* Применение моделей интерливинга для описания интрузионного расслоения на фронтах глубинной полярной воды Евразийского бассейна (Арктика) // Океанология. 2014. Т. 54. С. 594–604.
5. *Кузьмина Н.П.* Об одной гипотезе образования крупномасштабных интрузий в Арктическом бассейне // Фундаментальная и прикладная гидрофизика. 2016. Т. 9, № 2. С. 15–26.
6. *Kuzmina N.P.* Generation of large-scale intrusions at baroclinic fronts: an analytical consideration with a reference to the Arctic Ocean // Ocean Sci. 2016. V. 12. P. 1269–1277.
doi: 10.5194/OS–12–1269–2016
7. *Журбас Н.В.* О спектрах собственных значений в модельной задаче описания образования крупномасштабных интрузий в Арктическом бассейне // Фундаментальная и прикладная гидрофизика. 2018. Т. 11, № 1. С. 40–45. doi: 10.7868/S2073667318010045
8. *Eady E.T.* Long waves and cyclone waves // Tellus. 1949. V. 1, N3. P. 33–52.
9. *Кузьмина Н.П.*, *Скороходов С.Л.*, *Журбас Н.В.*, *Лыжков Д.А.* Описание возмущений океанских геострофических течений с линейным вертикальным сдвигом скорости с учетом трения и диффузии плавучести // Изв. РАН. Физика атмосферы и океана. 2019. Т. 55, № 2. С. 73–85. doi: 10.31857/S0002–351555273–85
10. *Stern M.E.* Lateral mixing of water masses // Deep Sea Res. Part A. 1967. V. 14. P. 747–753.
11. *Kuzmina N.P.* On the parameterization of interleaving and turbulent mixing using CTD data from the Azores Frontal Zone // J. Mar. Syst. 2000. V. 23. P. 285–302.

12. *Журбас В.М.*, *Кузьмина Н.П.*, *Озмидов Р.В., Голенко Н.Н.*, *Пака В.Т.* О проявлении процесса субдукции в термохалинных полях вертикальной тонкой структуры и горизонтальной мезоструктуры во фронтальной зоне Азорского течения // Океанология. 1993. Т. 33, № 3. С. 321–326.
13. *Журбас В.М.*, *Пака В.Т.*, *Голенко М.Н.*, *Корж А.О.* Оценка трансформации распространяющейся на восток соленой воды на Слупском пороге Балтийского моря по данным микроструктурных измерений // Фундаментальная и прикладная гидрофизика. 2019. Т. 12, № 2. С. 43–49. doi: 10.7868/S2073667319020060
14. *Вяли Г.*, *Журбас В.М.*, *Лаанеметс Я.*, *Липс У.* Кластеризация плавающих частиц из-за субмезомасштабной динамики: модельное исследование для Финского залива Балтийского моря // Фундаментальная и прикладная гидрофизика. 2018. Т. 11, № 2. С. 21–35. doi: 10.7868/S2073667318020028
15. *Haine T.W.*, *Marshall J.* Gravitational, symmetric, and baroclinic instability of the ocean mixed layer // J. Phys. Oceanogr. 1998. V. 28, N4. P. 634–658. doi: 10.1175/1520–0485(1998)028<0634: GSABIO>2.0.CO;2
16. *Thomas L.N.*, *Taylor J.R.*, *D'Asaro E.A.*, *Lee C.M.*, *Klymak J.M.*, *Shcherbina A.* Symmetric instability, inertial oscillations, and turbulence at the Gulf Stream front // J. Phys. Oceanogr. 2016. V. 46, N1. P. 197–217. doi: 10.1175/JPO-D-15–0008.1
17. *Taylor J.R.*, *Ferrari R.* On the equilibration of a symmetrically unstable front via a secondary shear instability // J. Fluid Mech. 2009. V. 622. P. 103–113. doi: 10.1017/S0022112008005272
18. *Bachman S.D.*, *Fox-Kemper B.*, *Taylor J.R.*, *Thomas L.N.* Parameterization of frontal instabilities. I: Theory for Resolved Fronts // Ocean Model. 2017. V. 109. P. 72–95. doi: 10.1016/j.ocemod.2016.12.003
19. *McIntyre E.* Diffusive destabilization of the baroclinic circular vortex // Geophys. Fluid Dyn. 1970. V. 1. P. 19–57. doi: 10.1080/03091927009365767
20. *Stone P.H.* On non-geostrophic baroclinic stability // J. Atmos. Sci. 1966. V. 23, N4. P. 390–400.
21. *Hoskins B.J.* The role of potential vorticity in symmetric stability and instability // Q. J.R. Met. Soc. 1974. V. 100. P. 480–482.
22. *Boccaletti G.*, *Ferrari R.*, *Fox-Kemper B.* Mixed Layer Instabilities and Restratification // J. Phys. Oceanogr. 2007. V. 37. P. 2228–2250. doi: 10.1175/JPO3101.1
23. *Kuzmina N.*, *Rudels B.*, *Stipa T.*, *Zhurbas V.* The Structure and Driving Mechanisms of the Baltic Intrusions // J. Phys. Oceanogr. 2005. V. 35, N6. P. 1120–1137. doi: 10.1175/JPO2749.1
24. *Ruddick Barry.* Intrusive Mixing in a Mediterranean Salt Lens — Intrusion Slopes and Dynamical Mechanisms // J. Phys. Oceanogr. 1992. V. 22. P. 1274–1285. doi: 10.1175/1520–0485(1992)022<1274: IMIAMS>2.0.CO;2

References

1. *Kuzmina N.P.*, *Rodionov V.B.* Influence of baroclinicity on formation of thermohaline intrusions in oceanic frontal zones. *Izv. Akad. Nauk USSR, Atmos. Oceanic Ph*ys. 1992, 28, 804–810.
2. *May B.D.*, *Kelley D.E.* Effect of baroclinicity on double-diffusive interleaving. *J. Phys. Oceanogr.* 2007, 27, 1997–2008.
3. *Kuzmina N.P.*, *Zhurbas V.M.* Effects of double diffusion and turbulence on interleaving at baroclinic oceanic fronts. *J. Phys. Oceanogr.* 2000, 30, 3025–3038.
4. *Kuzmina N.P.*, *Zhurbas N.V.*, *Emelianov M.V.*, *Pyzhevich M.L.* Application of interleaving models for the description of intrusive layering at the fronts of deep polar water in the Eurasian basin (Arctic). Oceanology. 2014, 54, 5, 557–566.
5. *Kuzmina N.P.* About one hypothesis of generation of large-scale intrusions in the Arctic Ocean. *Fundam. Prikl. Gidrofiz.* 2016, 9, 2, 15–26 (in Russian).
6. *Kuzmina N.P.* Generation of large-scale intrusions at baroclinic fronts: an analytical consideration with a reference to the Arctic Ocean. *Ocean Sci.* 2016, 12, 1269–1277. doi: 10.5194/OS–12–1269–2016
7. *Zhurbas N.V.* On the eigenvalue spectra for a model problem describing formation of the large-scale intrusions in the Arctic basin. *Fundam. Prikl. Gidrofiz.* 2018, 11, 1, 40–45. doi: 10.7868/S2073667318010045
8. *Eady E.T.* Long waves and cyclone waves. *Tellus*. 1949, 1, 3, 33–52.
9. *Kuzmina N.P.*, *Skorokhodov S.L.*, *Zhurbas N.V.*, *Lyzhkov D.A.* Description of the perturbations of oceanic geostrophic currents with linear vertical velocity shear taking into account friction and diffusion of density. *Izv. Atmos. Oceanic Phys.* 2019, 55, 207–217. doi: 10.1134/S0001433819020117
10. *Stern M.E.* Lateral mixing of water masses. *Deep Sea Res.* Part A. 1967, 14, 747–753.
11. *Kuzmina N.P.* On the parameterization of interleaving and turbulent mixing using CTD data from the Azores Frontal Zone. *J. Mar. Syst.* 2000, 23, 285–302.
12. *Zhurbas V.M.*, *Kuzmina N.P.*, *Ozmidov R.V.*, *Golenko N.N.*, *Paka V.T.* On the manifestation of subduction in thermohaline fields of the vertical fine structure and horizontal mesostructure in the frontal zone of the Azores Current. *Okeanologiya*. 1993, 33, 3, 321–326 (in Russian).

13. *Zhurbas V.M.*, *Paka V.T.*, *Golenko M.N.*, *Korzh A.O.* Transformation of eastward spreading saline water at the Słupk Sill of the Baltic Sea: an estimate based on microstructure measurements. *Fundam. Prikl. Gidrofiz.* 2019, 12, 2, 43–49. doi: 10.7868/S2073667319020060
14. *Väli G.*, *Zhurbas V.M.*, *Laanemets J.*, *Lips U.* Clustering of floating particles due to submesoscale dynamics: a simulation study for the Gulf of Finland, Baltic Sea. *Fundam. Prikl. Gidrofiz.* 2018, 11, 2, 21–35. doi: 10.7868/S2073667318020028
15. *Haine T.W.*, *Marshall J.* Gravitational, symmetric, and baroclinic instability of the ocean mixed layer. *J. Phys. Oceanogr.* 1998, 28(4), 634–658. doi: 10.1175/1520–0485(1998)028<0634: GSABIO>2.0.CO;2
16. *Thomas L.N.*, *Taylor J.R.*, *D'Asaro E.A.*, *Lee C.M.*, *Klymak J.M.*, *Shcherbina A.* Symmetric instability, inertial oscillations, and turbulence at the Gulf Stream front. *J. Phys. Oceanogr.* 2016, 46, 1, 197–217. doi: 10.1175/JPO-D-15–0008.1
17. *Taylor J.R.*, *Ferrari R.* On the equilibration of a symmetrically unstable front via a secondary shear instability. *J. Fluid Mech.* 2009, 622, 103–113. doi: 10.1017/S0022112008005272
18. *Bachman S.D.*, *Fox-Kemper B.*, *Taylor J.R.*, *Thomas L.N.* Parameterization of frontal instabilities. I: Theory for Resolved Fronts. *Ocean Model.* 2017, 109, 72–95. doi: 10.1016/j.ocemod.2016.12.003
19. *McIntyre E.* Diffusive destabilization of the baroclinic circular vortex. *Geophys. Fluid Dyn.* 1970, 1, 19–57. doi: 10.1080/03091927009365767
20. *Stone P.H.* On non-geostrophic baroclinic stability. *J. Atmos. Sci.* 1966, 23, 4, 390–400.
21. *Hoskins B.J.* The role of potential vorticity in symmetric stability and instability. *Q.J.R. Met. Soc.* 1974, 100, 480–482.
22. *Boccaletti G.*, *Ferrari R.*, *Fox-Kemper B.* Mixed Layer Instabilities and Restratification. *J. Phys. Oceanogr.* 2007, 37, 2228–2250. doi: 10.1175/JPO3101.1
23. *Kuzmina N.*, *Rudels B.*, *Stipa T.*, *Zhurbas V.* The structure and driving mechanisms of the Baltic intrusions. *J. Phys. Oceanogr.* 2005, 35, 6, 1120–1137. doi: 10.1175/JPO2749.1
24. *Ruddick Barry.* Intrusive mixing in a Mediterranean salt lens — intrusion slopes and dynamical mechanisms. *J. Phys. Oceanogr.* 1992, 22, 1274–1285. doi: 10.1175/1520–0485(1992)022<1274: IMIAMS>2.0.CO;2